Nuclear Instruments and Methods in Physics Research A 766 (2014) 288–291

Contents lists available at ScienceDirect

Nuclear Instruments and Methods in Physics Research A

journal homepage: www.elsevier.com/locate/nima

Particle identification with the ALICE Time-Of-Flight detector at the LHC

A. Alici [a,b,*]

[a] Centro Fermi - Centro Studi e Ricerche e Museo Storico della Fisica "Enrico Fermi", Rome, Italy
[b] Sezione INFN, Bologna, Italy

ALICE Collaboration

ARTICLE INFO

Available online 23 May 2014

Keywords:
ALICE
Time-Of-Flight
MRPC

ABSTRACT

High performance Particle Identification system (PID) is a distinguishing characteristic of the ALICE experiment at the CERN Large Hadron Collider (LHC). Charged particles in the intermediate momentum range are identified in ALICE by the Time-Of-Flight (TOF) detector. The TOF exploits the Multi-gap Resistive Plate Chamber (MRPC) technology, capable of an intrinsic time resolution at the level of few tens of ps with an overall efficiency close to 100% and a large operation plateau. The full system is made of 1593 MRPC chambers with a total area of 141 m^2, covering the pseudorapidity interval $[-0.9,+0.9]$ and the full azimuthal angle.

The ALICE TOF system has shown very stable operation during the first 3 years of collisions at the LHC. In this paper a summary of the system performance as well as main results with data from collisions will be reported.

1. Introduction

The ALICE [1] experiment at the LHC investigates the properties of the strongly interacting matter at very high temperature that is created in high-energy Pb–Pb collisions. It also studies pp and p–Pb collisions both for comparison with Pb–Pb interactions and in physics areas where ALICE is complementary with other LHC experiments. Particle IDentification (PID) is a crucial aspect of the ALICE experiment and it is performed by combining different detecting systems [2].

One of the main detectors devoted to charged hadron identification in the central barrel is a large Time-Of-Flight (TOF) system [3], covering a cylindrical surface of 141 m^2 with an inner radius of 3.7 m, a polar acceptance of $|\theta-90^\circ|<45^\circ$ and a full coverage in the azimuthal angle. The TOF aims at 3σ π/K and K/p track-by-track separation for momenta up to 2.5 GeV/c and 4 GeV/c, respectively. This performance requires a Time-Of-Flight resolution (including start and stop times and reconstruction effects) better than 100 ps which may be achieved by means of the Multigap Resistive Plate Chamber (MRPC) [4,5] technology. The TOF detector consists of 1593 MRPCs arranged in 90 gas-tight modules. The whole structure is divided into 18 sectors in the azimuthal angle ϕ, each one containing a supermodule (SM) more than 9 m long; five modules are grouped in a line to form one SM.

In this paper the TOF performance during the pp, the Pb–Pb and the p–Pb data taking at the LHC is described; more details on results and figures can be found in Ref. [6].

2. ALICE-TOF MRPCs: design and behaviour

The MRPCs are robust and simple gaseous parallel-plate avalanche detectors that implement electrodes made of a material with a high volume resistivity. The very good time resolution of MRPCs is due to the strong uniform electric field, which starts the avalanche process immediately after primary ionization is deposited in the gas volume; thus the resolution is determined mainly by the avalanche statistics and in first approximation it improves by increasing the strength of the electric field [7]. Tiny gaps allow us to have intense electric fields preventing avalanches growing too big and eventually developing to streamers [8]; a series of many gas gaps guarantees a high efficiency. The MRPC was chosen being the only technology able to fulfill the three major requirements for such large area, small granularity TOF array, i.e. an extremely high time resolution, a good detection efficiency and cost effectiveness. Test beam results may be found in Refs. [9,10],

* Correspondence address: Centro Fermi - Centro Studi e Ricerche e Museo Storico della Fisica "Enrico Fermi", Rome, Italy.
E-mail address: alici@bo.infn.it

http://dx.doi.org/10.1016/j.nima.2014.05.059
0168-9002/

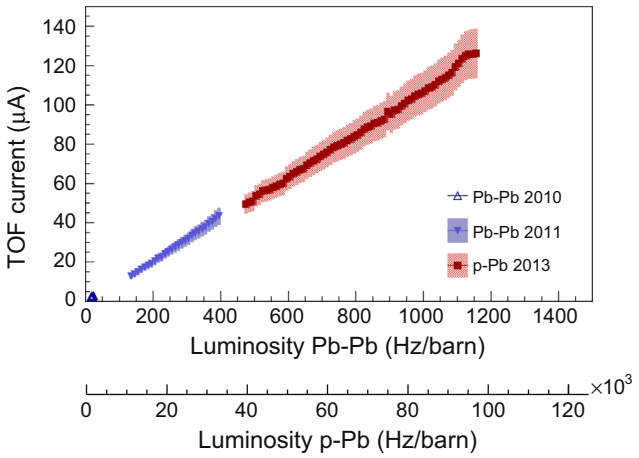

Fig. 1. TOF current vs. luminosity in Pb–Pb and p–Pb. The bands represent a safety 10% error since measurements were affected by fill-dependent beam conditions.

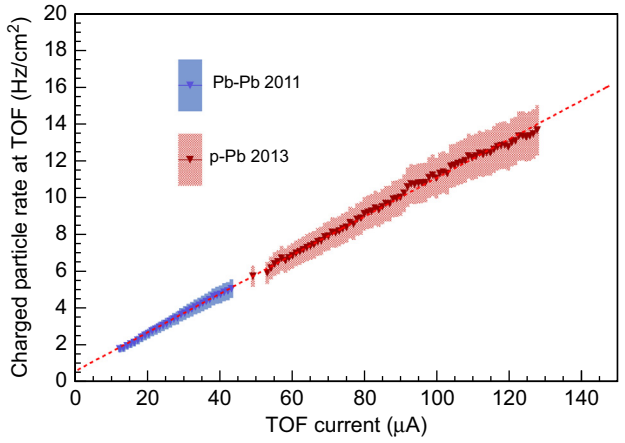

Fig. 2. TOF estimated rate vs. HV current. The bands represent a safety 10% error since measurements were affected by fill-dependent beam conditions. The dashed line is the linear fit to the 2013 data.

where the performance of a sample of MRPCs has been measured to be well within the ALICE requirements. A detailed overview of the ALICE-TOF MRPCs design as well as description of the detector construction procedure and quality tests can be found in Ref. [10].

The behaviour of the MRPCs was very stable along the first 3 years of the LHC operation. The TOF current, defined as the sum over all MRPCs of the average of the two currents (positive and negative) measured at the anode and at the cathode and representing the total current flowing across the MRPCs, increased linearly with the LHC luminosity (Fig. 1), with no sign of deviations related to the occurrence of abnormal noise current. The two horizontal axes, relative to different collisions, are aligned to the same detector load considering the average track multiplicity and the ALICE interaction rate. The maximum current drawn by the full TOF during the first 3 years of operation was less than 100 nA per MRPC (less than 1 $\mu A/m^2$). The total integrated TOF charge during LHC Run 1 (2010–2013) has been evaluated to be of the order of 0.2 mC/cm^2 (detectors were validated up to 24 mC/cm^2 [11]).

Considering the interaction rate at ALICE and the TOF hit multiplicity per event it is possible to estimate the average rate of particles in the detector as a function of the TOF current. The calculation is shown in Fig. 2 and it indicates a maximum fluence rate at TOF of $\approx 14\,Hz/cm^2$. Considering the two plots in Figs. 1 and 2 it is possible to extrapolate the fluence rate at TOF to the luminosity foreseen in the ALICE upgrade beyond 2018 (5000 Hz/barn [12] for Pb–Pb at $\sqrt{s_{NN}} = 5.5$ TeV). The expected value will be 90 Hz/cm^2: when compared to test beam results [13] it indicates that also in the high-luminosity LHC period the MRPCs are expected to operate without loss in performance. From Fig. 2 it is also possible to estimate the charge induced by traversing particles inside the MRPCs, which is 6 pC on average.

Also the MRPC detection efficiency, evaluated using the ratio between TOF matched tracks with those reconstructed in the ALICE central tracking detectors, has shown a stable behaviour with time [6]. Comparing data and Monte Carlo simulations, an MRPC efficiency of 98.5% in good agreement with test beam results on readout pad scanning has been estimated.

The small current and the low noise rate of the MRPCs ($\approx 0.5\,Hz/pad$ without beam) allow the TOF to be used as a trigger detector; taking advantage of its large coverage, fine granularity and fast signals, the TOF system has been extensively used as a trigger detector during different periods of the ALICE commissioning and data taking.

3. PID analysis

3.1. Event time determination

A TOF measurement yields the velocity of a charged particle by measuring the particle Time-Of-Flight t (defined as the difference between the arrival time measured by the TOF and the event time which is estimated event by event) over a given distance along the track trajectory L. Event time determination is made in ALICE by means of the T0 detector [14]. However, due to the detector acceptance, especially in pp collisions, no signals are observed by the T0 for a fraction of the events; this is why an alternative method using the particle arrival times at the TOF, when at least three tracks have an associated TOF signal, was developed. This method is based on a combinatorial algorithm which compares the measured TOF times to the expected times of the tracks, assuming a common event time t_{ev}. This latter quantity is obtained from a χ^2-minimization procedure. In detail, for a given track j, the event time is determined using all the other tracks in the event and evaluating the following χ^2 expression for all possible combinations of masses ($m_i, i = \pi$, K, p):

$$\chi^2 = \sum_{n_{tracks}} \frac{((t_{TOF} - t_{ev}) - t_{exp}(m_i))^2}{\sigma^2_{TOF} + \sigma^2_{t_{exp}}} \quad (1)$$

where the sum is over all tracks matched at TOF other than j, t_{TOF} is the track measured time and t_{exp} is the expected time with the mass hypothesis i. σ_{TOF} and $\sigma_{t_{exp}}$ are the corresponding errors. The combination that minimizes the χ^2 yields t_{ev} which is then subtracted from the TOF time associated with track j. This procedure, which is repeated for each track in the event, ensures that the measured event time is always independent of the TOF measured time of the track, thus avoiding possible biases in the determination of t_{ev}. In the physics analysis the event time is determined combining the event time estimated by the T0 detector and by the TOF tracks, weighted by the respective resolutions. When none of the two measurements is available the event time is taken as the average obtained during the run, of course with a much worse resolution on t_{ev}.

3.2. Timing calibration and time resolution

In the determination of the total TOF resolution σ_{TOF} the following contributions have to be considered:

$$\sigma^2_{TOF} = \sigma^2_{MRPC} + \sigma^2_{elec} + \sigma^2_{clock} + \sigma^2_{cal} \quad (2)$$

where σ_{MRPC} is the MRPC intrinsic time resolution, σ_{elec} combines the intrinsic time jitter of the amplification electronics (20 ps) and

of the time-to-digital conversion (30 ps) and σ_{clock} accounts for the uncertainties arising from the distribution of the digital clock from the LHC to the experiments and through the electronics chain (15 ps). Finally, a contribution σ_{cal} includes all effects that can be parametrized and that are thus accessible to calibration methods in order to be minimized.

The TOF time calibration is based on the determination of three components: (i) a global offset, which is common to all the channels, (ii) a channel-by-channel offset and (iii) a time-slewing correction at the channel level.

The need to sample the global offset in time comes from the observation of a time shift in the LHC clock phase, which results in a non-constant offset in the measured time of flight. The global offset is derived by measuring the arrival times of flight for particles with momentum $p > 0.5$ GeV/c and by comparing them to the expected times in the pion mass hypothesis (10 min samples); the corresponding distribution is fitted with a Gaussian function whose mean corresponds to the global channel offset.

The channel-by-channel offset calibration accounts for the delays introduced in the measured times of flight by the cable lengths and by the electronics. Several million events are used for pp collisions, collected over several days of data taking.

The time-slewing correction, that is applied on channel-by-channel basis, makes use of the correlation between the measured time and the signal width. To reach the very high statistics necessary for this two-dimensional calibration, data are collected over periods of several months. This large integration in time is allowed by the absence of significant changes with time, thus thanks to the high stability of system.

After the above three calibrations, it is possible to evaluate the TOF performance in terms of time resolution by considering the difference between the measured time of flight and the pion time expectation for tracks with a momentum in the range $0.95 < p < 1.05$ GeV/c (the contribution from tracking is negligible for this momentum range [6]) and using the event time determination performed by the TOF itself. The distribution is fitted with a Gaussian function, whose width is the convolution of the TOF time resolution σ_{TOF} and the event time resolution $\sigma_{t_{\text{ev}}}$. Since the TOF t_{ev} resolution is expected to scale with the square root of the number of tracks used ($\sigma_{t_{\text{ev}}} = A/\sqrt{n_{\text{tracks}}}$), the measured total resolution can be plotted versus n_{tracks} and fitted according to this expression. Red solid points in Fig. 3, obtained for p–Pb collisions, represent the width of such Gaussian fits and indicate an asymptotic TOF time resolution of 80 ps. The inset shows an example of a Gaussian fit for a track multiplicity on TOF in excess of 20: the distribution has a tail on the right, which was not observed during test beams, and might be related to mis-association when TPC tracks are matchable with more than one TOF hit, due to the finite resolution of the tracking at TOF (20% of tracks have more than one hit on TOF). This effect is currently under investigation. The impact on PID reflects on a reduced efficiency when applying for example a 2σ inclusive cut, but it is negligible at 3σ. The detector response includes a modeling of the tails in the Monte Carlo.

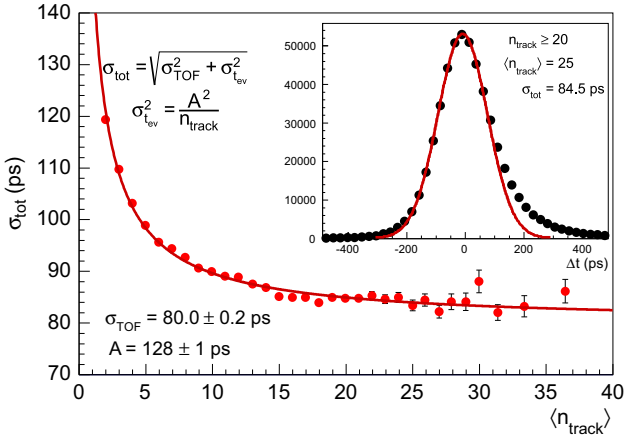

Fig. 3. Total time resolution for pion tracks on TOF with $0.95 < p < 1.05$ GeV/c as a function of the number of tracks used to define the TOF event time. Data refer to p–Pb collisions. The inset shows the original distribution for a track multiplicity on TOF > 20 which corresponds to an average of 25. (For interpretation of the references to colour in this figure caption, the reader is referred to the web version of this paper.)

3.3. Particle identification with TOF

Particles are identified in the TOF by comparing the measured time of flight to the expected time for a given particle species. The cut is expressed in units of the estimated time resolution, assuming a Gaussian description of the response function of the detector, in the following way:

$$\delta_i = \frac{t_{\text{TOF}} - t_{\text{ev}} - t_{\text{exp}}(m_i, p, L)}{\sigma_{\text{tot}}(p, m_i, t_{\text{ev}})} \tag{3}$$

where t_{exp} is the expected time for a particle of mass m_i, momentum p and track length L reaching the TOF. The resolution function $\sigma_{\text{tot}}(p, m_i, t_{\text{ev}})$ takes into account, summing in quadrature, the intrinsic TOF detector contribution ($\sigma_{\text{TOF}} \approx 80$ ps as explained in Section 3.2), the uncertainty on the event time of the collision and the uncertainty due to the tracking and reconstruction. The δ variable is then used to implement simple 2 or 3σ cuts, depending on the requirements of the specific analysis. The goodness of the calibration procedures as well as the understanding of the detector response and parametrization of its resolution is confirmed by monitoring the average values and pulls of the distribution of this variable (expected around 0 and 1, respectively). As an example, the distribution of this variable as a function of momentum for the kaon hypothesis is shown in Fig. 4. Pions and protons are also visible as well as the region where pions start affecting the purity of a selected kaon sample. Each momentum slice has been fitted with a Gaussian fit bound to $[-2,2]$ values and the resulting mean and width of the distribution are plotted as black and red points, respectively. By construction, the fitted width corresponds to the pull of the distribution of the δ variable. In the range where there is no contamination from pions the values are in nice agreement with the expected values for mean and pull of the variable (represented by the dashed lines) validating the description of the resolution function.

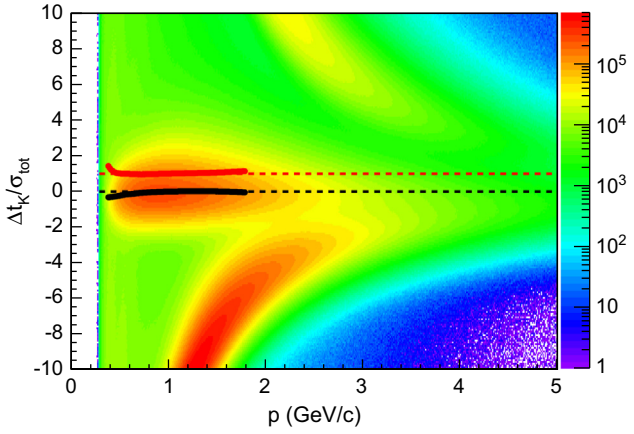

Fig. 4. For real data, TOF deviations versus the track momentum considering the kaon expected time. The accumulation bands corresponding to pions and protons are clearly visible. Points indicate the average (black) and the width (red) of the distribution for each momentum bin. (For interpretation of the references to colour in this figure caption, the reader is referred to the web version of this paper.)

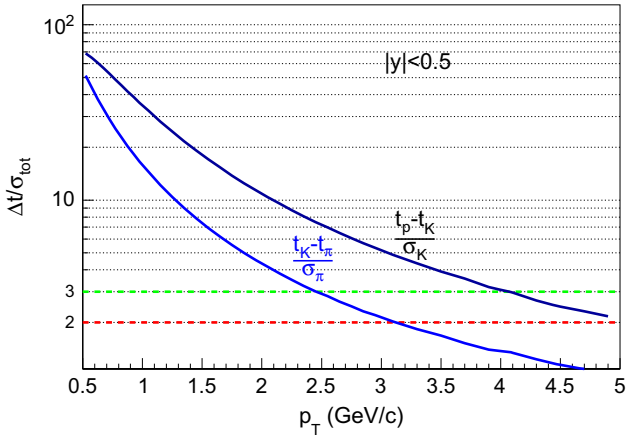

Fig. 5. Measured separation power of the TOF for kaon–pion and proton–kaon as a function of p_T.

In Fig. 5 the separation power of the TOF for kaon–pion and proton–kaon as a function of transverse momentum is shown. Usually this is shown as a function of total momentum p as in Fig. 4; however, since most physics results are reported in transverse momentum bins, here the separation power in p_T bins is reported, averaging the momentum-dependent response over the range $|y| < 0.5$. The design 3σ separation for K/π up to 2.5 GeV/c and for p/K up to 4 GeV/c has been clearly achieved.

3.4. Analyses with TOF

Currently the TOF detector contributes to a large set of physics analyses in ALICE for all LHC colliding systems and energies. Here follows a non-exhaustive list of topics where TOF is used:

- production of π, K, p, where tracks are selected by applying a 3σ cut on the Time-Of-Flight, then particle yields are extracted with a statistical method [15];
- production of light (anti)nuclei, where the mass measurement with the TOF is needed to separate candidates for which the dE/dx bands in the TPC are overlapping [14];
- production of hadronic resonances, where the resonances are identified via their main decay channels (for example, $K^* \to \pi^{\pm} K^{\mp}$ or $\phi \to K^+ K^-$) and TOF is used to identify the decay daughters [16];
- production of heavy-flavour electrons. In this analysis the most important role in particle identification is played by the TPC. The information provided by the TOF detector is used to resolve the ambiguities in the crossing regions of the TPC electron, kaon and proton lines [17];
- production of charmed mesons and baryons, where candidates are selected by measuring their decay vertex and the PID is used to provide background rejection especially in the low-momentum region [18,19];
- exclusive production of vector mesons in ultra-peripheral Pb–Pb collisions (UPC), where TOF also provides the trigger [20];
- elliptic-flow of identified charged hadrons [21].

4. Conclusions

The ALICE TOF system, based on the MRPC technology, is a large and high-performance detector. It has shown very stable operation during the first 3 years of collisions at the LHC. Currents and rates behaved as expected during the periods of data taking with beam, with no sign of degradation of the detector, allowing also the TOF to be used as a trigger detector.

The data demonstrate that the TOF can provide 3σ K/π separation up to 2.5 GeV/c and p/K separation up to 4 GeV/c with full azimuthal coverage in the ALICE central barrel. The TOF PID is extensively and successfully exploited in many analyses in ALICE for all LHC colliding systems and energies.

References

[1] ALICE Collaboration, Journal of Physics G: Nuclear and Particle Physics 30 (2004) 1517; Journal of Physics G: Nuclear and Particle Physics 32 (2006) 1295; IOP—Journal of Instrumentation 3 (2008) S08002.
[2] ALICE Collaboration, ALICE: Physics Performance Report, vol. II, Journal of Physics G 32 (2006) 1295–2040.
[3] ALICE Collaboration, Addendum to TOF Technical Design Report, CERN/LHCC 2002-016.
[4] E. Cerron-Zeballos, et al., Nuclear Instruments and Methods in Physics Research Section A 374 (1996) 132.
[5] P. Fonte, A. Smirnitski, M.C.S. Williams, Nuclear Instruments and Methods in Physics Research Section A 433 (2000) 201.
[6] A. Akindinov, et al., The European Physical Journal Plus 128 (4) (2013).
[7] W. Riegler, C. Lippmann, R. Veenhof, Nuclear Instruments and Methods in Physics Research Section A 500 (2003) 144.
[8] J. Meek, Physical Review 57 (1940) 722.
[9] A. Akindinov, et al., Nuclear Instruments and Methods in Physics Research Section A 532 (2004) 611.
[10] A. Akindinov, et al., Nuovo Cimento B 124 (2009) 235.
[11] A. Alici, et al., Nuclear Instruments and Methods in Physics Research Section A 579 (2007) 979.
[12] ALICE Collaboration, CERN-LHCC-2012-012/LHCC-I-022 September 7, 2012.
[13] A. Akindinov, et al., Nuclear Instruments and Methods in Physics Research Section A 490 (2002) 58.
[14] ALICE Collaboration, Performance of the ALICE Experiment at the CERN LHC, arXiv:1402.4776v2.
[15] ALICE Collaboration, Physical Review Letters 109 (2012) 252301.
[16] ALICE Collaboration, European Physical Journal C 72 (2012) 2183.
[17] ALICE Collaboration, Physical Review D 86 (2012) 112007.
[18] ALICE Collaboration, Journal of High Energy Physics 1207 (2012) 191.
[19] ALICE Collaboration, Physics Letters B 718 (2012) 279.
[20] ALICE Collaboration, Physics Letters B 718 (2013) 1273.
[21] F. Noferini, Nuclear Physics A 904–905 (2013) 483c.